Am J Transl Res 2026;18(3):2489-2506
www.ajtr.org /ISSN:1943-8141/AJTR0170388

Original Article

Jiangfu Fuwei granules alleviate chronic atrophic gastritis by suppressing angiogenesis through the PI3K-AKT-HIF1α pathway

Yuqing Bi[1], Yanchun Chen[1], Jimei Jiang[1], Wangqi Mao[1], Xiao Zhang[1], Jiayi Liu[1], Xin Zhao[2], Yueqiu Dong[1], Yueqing Cai[1], Mei Li[3], Xiang Li[2], Yunpeng Luan[2], Liyun Jiang[1]

[1]Department of Pi-Wei Disease, The Third Affiliated Hospital of Yunnan University of Chinese Medicine, Kunming 650500, Yunnan, China; [2]Department of Pi-Wei Disease, The First Affiliated Hospital of Yunnan University of Chinese Medicine, Kunming 650021, Yunnan, China; [3]Department of Oncology, The First Affiliated Hospital of Kunming Medical University, Kunming 650118, Yunnan, China

Received November 29, 2025; Accepted January 28, 2026; Epub March 15, 2026; Published March 30, 2026

Abstract: Objective: Jiangfu Fuwei granules (JFFW) are a widely used clinical prescription for the treatment of chronic atrophic gastritis (CAG), but the underlying molecular mechanism remains to be explored. This study aimed to elucidate the therapeutic mechanism of JFFW in alleviating CAG. Methods: A CAG mouse model was established using a combined approach, and the mice were treated with JFFW for six weeks. Network pharmacology was used to screen for active ingredients and signaling pathways. Subsequently, *in vivo* experiments were conducted to verify the predicted mechanisms, including histologic evaluation, enzyme-linked immunosorbent assay, and immunohistochemical analysis. Furthermore, molecular docking was used to simulate the interaction between key active compounds and core protein targets. Results: *In vivo* experimental results demonstrated that JFFW effectively reversed gastric mucosal thinning and glandular loss in CAG mice. This treatment significantly restored serum pepsinogen levels and downregulated the expression of inflammatory cytokines, specifically interleukin-6, interleukin-1β, and tumor necrosis factor-α. Network pharmacology analysis identified 224 bioactive compounds and predicted the phosphoinositol 3-kinase (PI3K)-protein kinase B (AKT)-hypoxia-inducible factor 1-α (HIF1α) signaling pathway as a key target. Immunohistochemical results confirmed that JFFW treatment significantly inhibited the protein expression of phosphorylated AKT and HIF1α. Furthermore, reduced CD31 staining occurred consistent with a decrease in microvessel density. Molecular docking analysis further confirmed that the main components of JFFW had a good binding affinity to PI3K protein. Conclusion: The therapeutic effect of JFFW on CAG is mainly achieved by inhibiting the PI3K-AKT-HIF1α signaling pathway, thereby suppressing abnormal angiogenesis and gastric inflammation.

Keywords: Jiangfu Fuwei granules, chronic atrophic gastritis, network-based pharmacology, PI3K-AKT-HIF1α pathway, angiogenesis

Introduction

Chronic atrophic gastritis (CAG), also known as chronic gastritis, is characterized by a reduction and disappearance of glandular tissue within the lamina propria. This degeneration is caused by repeated damage to the epithelial gastrointestinal region and may be associated with intestinal metaplasia and/or pseudopolar metaplasia [1, 2]. Recent studies have shown a strong correlation between inflammatory events and cancer-causing changes, suggesting that these phenomena play a crucial role in the development of gastric cancer (GC). Correa's case describes how gastric mucosal inflammation leads to atrophy of mucosal glands, a stage preceding intestinal metaplasia, intraepithelial neoplasia, and even gastric cancer [3, 4]. Therefore, CAG can be considered a precancerous lesion of gastric cancer and is positively correlated with the incidence of GC [5, 6]. Early diagnosis and treatment of CAG are of profound significance for the prevention of GC. In addition, most patients with CAG experience some clinical symptoms, including postprandial upper abdominal fullness or pain, belching, and acid

https://doi.org/10.62347/ABOM6140

reflux (or heartburn). Most patients may also experience psychologic symptoms such as forgetfulness, anxiety, and depression. These symptoms often recur, severely reducing patients' quality of life [7]. Currently, the prevention and management of CAG has become an important topic of concern for clinicians and researchers worldwide. It has been reported that Helicobacter pylori proliferation, bile reflux, autoimmune reactions, and other physical or chemical damaging factors may be pathogenic factors of CAG. Clinical treatment for CAG mainly includes eradication of Helicobacter pylori infection, protection of the gastric mucosa, and vitamin supplementation. However, the effectiveness of these treatments is limited, with a high relapse rate after discontinuation, and some side effects [8]. Therefore, more effective treatments are needed to improve clinical symptoms, reduce relapse rates, improve patients' quality of life, and reverse the pathologic progression of CAG.

Traditional Chinese medicine (TCM) has been used in the treatment of CAG, with fewer side effects and significant advantages [9]. Jiangfu Fuwei Granules (JFFW) is a TCM formula invented by Professor Jiang Liyun, a TCM expert in Yunnan Province. Based on the academic thought of the Yunnan Fuyang School, it is used to treat CAG caused by spleen and kidney yang deficiency and liver cold qi stagnation. In 2021, the formula obtained a national patent [10]. Its main ingredients include Monkshood (Fuzi), Dried Ginger (Ganjiang), Dark Plum (Wumei), Evodia Rutaecarpa (Wuzhuyu), Angelica Root (Danggui), Chuanxiong Rhizoma (Chuanxiong), Cinnamomum Cassia (Rougui), Amomum Fruit (Sharen), Phellodendron Bark (Huangbai). The efficacy of this formula is to warm and tonify the spleen and kidney, warm the liver and stomach, and regulate qi and blood circulation.

Modern drug research shows that Radix Aconitum Lateralis Preparata (Fuzi) contains aconitine, mesaconitine and hypaconitine diester alkaloids, which can affect leukocyte chemotaxis, regulate prostaglandin metabolism, and may have anti-inflammatory effects [11]. Gingerol is the active ingredient of Zingiberis Rhizoma (ganjiang), which has strong antioxidant and anti-inflammatory effects in relieving gastrointestinal spasms and inflammation. Zingiberis Rhizoma extract can also neutralize gastric acid and protect the gastric mucosa [12]. Although JFFW has shown therapeutic value in clinical practice, its mechanism of action in treating CAG is still poorly understood. With the development of network pharmacology, a new drug development method has emerged. Based on the research results of multiple disciplines such as systems biology, multipharmacology and multiomics, it can study the complexity between different drug components, targets, diseases and molecular pathways, thereby explaining the mechanism of action of drugs in the human body [13, 14]. In view of this, the current study aimed to construct a mouse model of CAG using composite modeling technology, and then use it to study the therapeutic effect of JFFW. This study also aimed to reveal the mechanism of action of JFFW using network pharmacology as a framework. This study will comprehensively evaluate the therapeutic effect through *in vivo* experiments and molecular docking to verify the research results and enhance the credibility of the conclusions.

Materials and methods

Animals and treatment

Male SPF-grade mice were purchased from SPF (Beijing) Biotechnology Co., Ltd. Ethical approval for this study was obtained from the Ethics Committee of Yunnan Provincial Hospital of Traditional Chinese Medicine (Approval No.: DW-2024-064). Mice were acclimatized for one week under the following conditions: temperature 24 ± 2°C, relative humidity 45%-55%, and a 12-hour light-dark cycle. Mice were randomly divided into four groups of seven mice each: Group I (normal control group), Group II (CAG model group), Group III (JFFW at 6.89 g/kg, provided by the Preparation Room of the Third Affiliated Hospital of Yunnan University of Traditional Chinese Medicine), and Group IV (Morodan (MLD) group, at 0.72 g/kg, purchased from Handan Pharmaceutical Co., Ltd., batch number Z20090013).

Mice in Group I had free access to food and water, while mice in Groups II-IV had free access to a 0.05% N-methyl-N'-nitro-N-nitrosoguanidine (MNNG; CAS: 7025-7, batch number M105583, Shanghai Aladdin Biochemical Technology Co., Ltd.) solution (180 μg/mL). They were also fed a diet containing 0.05%

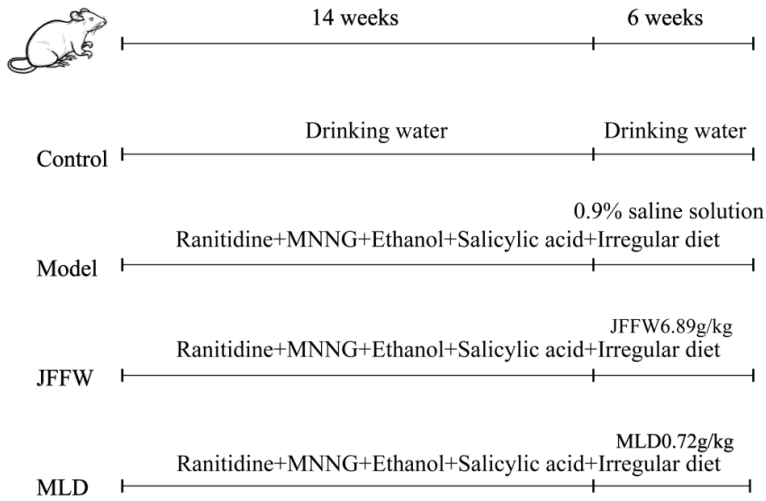

Figure 1. Schematic overview of the experimental design. Abbreviations: JFFW: Jiangfu Fuwei Granules; MLD: Morodan; MNNG: N-methyl-N'-nitro-N-nitrosoguanidine.

ranitidine (batch number 20240709, SPF (Beijing) Biotechnology Co., Ltd.) for 2 days, followed by fasting for 14-16 hours. After fasting, the mice were administered 20% anhydrous ethanol (batch number 20241101, Tianjin Damao Chemical Reagent Factory) and 2% sodium salicylate (product number R007062, Shanghai E&N Chemical Technology Co., Ltd.) solution by gavage. After 13 weeks, two mice were randomly selected for histopathologic analysis, confirming the successful establishment of a CAG model. After successful modeling, mice in each group received gavage with the corresponding drugs for 6 weeks (the control group and the CAG model group received physiological saline by gavage). After the last administration, all mice were fasted for 12 hours, followed by blood collection via o-orbital sinus puncture under anesthesia with 1% pentobarbital sodium (50 mg/kg, i.p.) to reduce pain. After the blood samples were allowed to stand for 4 hours, they were centrifuged at 3000 rpm for 15 minutes. The supernatant was collected and stored at -80°C for further analysis. Subsequently, while the mice were still under deep anesthesia, they were euthanized by cervical dislocation to ensure a humane endpoint, and gastric tissue was collected. A portion of the gastric tissue was rinsed with normal saline at 4°C, and excess moisture was absorbed with filter paper. Then, it was preserved with tissue fixative (Batch No. GP24103092070, Wuhan Servicebio Technology Co., Ltd.), quickly frozen in liquid nitrogen for 10-20 minutes, and stored at -80°C. Meanwhile, the remaining gastric tissue was treated with 4% neutral buffered formalin at room temperature for 24 hours for subsequent H&E staining. The modeling and drug administration process is illustrated in **Figure 1**.

Histologic analysis

Gastric tissues excised from mice were preserved in 4% formaldehyde solution for 24 hours. Subsequently, the tissue was dehydrated using ethanol and xylene. After this step, the specimens were embedded in paraffin and cut into 4-5 μm sections. These slides were then stained with hematoxylin and eosin (H&E). The stained tissue sections were observed under an optical microscope. Gastric mucosal samples from each group of mice were analyzed, and images were taken from three randomly selected fields of view at 10× magnification to assess inflammation and atrophy.

Inflammation was scored on a 0-3 scale: 0 indicated no inflammatory cell infiltration; 1 indicated infiltration below the lamina propria; 2 indicated infiltration exceeding half the mucosal thickness; 3 indicated infiltration extending to the epithelial gland layer, covering the entire mucosa.

The degree of atrophy was assessed according to the following criteria: 0 point indicated no reduction in gastric mucosal glands; 1 point indicated a reduction in intrinsic glands of no more than one-third of the original glands; 2 points indicated a reduction in glands between one-third and two-thirds; and 3 points indicated a significant reduction in glands, exceeding two-thirds.

Enzyme-linked immunosorbent assay (ELISA)

Following the instructions of the ELISA kit (Wuhan Servicebio Technology Co., Ltd.), inflammatory factors such as IL-6, IL-1β, TNF-α, PGI, and PGII in mouse serum were assessed.

Immunohistochemistry analysis (IHC)

Gastric tissue specimens were first fixed with 10% formaldehyde solution, then paraffin-embedded and sectioned. The specimens were dewaxed and rehydrated using a series of concentrations of ethanol. Antigen retrieval was performed using citrate buffer containing citric acid (Product No. G1202, Wuhan Servicebio Technology Co., Ltd.) via microwave for 16 minutes. After natural cooling, the tissue was rinsed three times for 5 minutes each time in phosphate-buffered saline (PBS; Product No. G0002, Wuhan Servicebio Technology Co., Ltd.). Subsequently, it was treated with 3% hydrogen peroxide solution for 25 minutes at room temperature in the dark. To ensure uniform coverage of the tissue sections, 3% bovine serum albumin solution was added to the histochemically stained areas and incubated at room temperature for 30 minutes for blocking. The samples were incubated overnight at 4°C, during which time they were treated with the following antibodies: rabbit polyclonal anti-P-AKT antibody (Servicebio, GB150002, dilution 1:200), rabbit polyclonal HIF-1α antibody (Servicebio, GB111339, dilution 1:100), and rabbit polyclonal anti-CD31 antibody (Servicebio, GB11063-2, dilution 1:600). Finally, the sections were treated with horseradish peroxidase (HRP)-labeled goat anti-rabbit secondary antibody (Servicebio, GB23303, dilution 1:200) and counterstained with hematoxylin.

Microscopic images were obtained. The immunostaining scoring criteria were based on the proportion and intensity of positive staining areas: unstained cells were scored 0 point; light yellow cells were scored 1 point; cells that were moderately yellow or brownish (without background) or dark brown but with a light brown background were classified as moderately positive and scored 2 points; cells that showed a strong positive response with dark brown coloration and no background staining scored 3 points.

The scoring criteria for the proportion of positive areas were as follows: 1 point for 1-10% positivity, 2 points for 11-50% positivity, 3 points for 51-80% positivity, and 4 points for more than 80% positivity. The overall score was obtained by multiplying the positive staining intensity by the corresponding proportion of positive areas. For each sample, five random fields of view were observed under a 200× magnification.

Microvessel density labeled by CD31 (CD31-MVD) was assessed using the Weidner method. Initially, three regions with the highest number of MVD were selected under low magnification. Subsequently, the number of microvessels in each region (brown-stained endothelial cells or endothelial cell clusters) was counted under high magnification, and the average value was defined as the CD31-MVD value for the sample.

Mechanism of JFFW in treating CAG based on network pharmacology

Potential targets of compounds in JFFW and targets associated with CAG: In the Traditional Chinese Medicine Systems Pharmacology Database and Analysis Platform (TCMSP, https://old.tcmsp-e.com/tcmsp.php), search criteria were set to search for the 14 Chinese herbal components of JFFW (monkshood, dried ginger, evodia rutaecarpa, cinnamomum cassia, phellodendron bark, amomum fruit, dark plum, chuanxiong, bergamot, angelica root, zedoary, chicken gizzard lining, and licorice) to obtain the potential active ingredients of the formula. The molecular names of each active ingredient were entered into the PubChem database to obtain their simplified linear input specification (SMILES) structural formulas. The obtained SMILES structural formulas were imported into the Swiss Target Prediction Database (STP, http://www.swisstargetprediction.ch/) to predict the potential targets corresponding to the active ingredients. For active ingredients whose targets were not found in the STP database, relevant targets were supplemented by searching the TCMSP database. Subsequently, all potential target information was submitted to the UniProt (https://www.uniprot.org/) general protein resource database for target name standardization.

Using “chronic atrophic gastritis” as the search term, disease-related targets were searched and screened in four databases: OMIM (https://omim.org/), PharmGKB (https://www.pharmgkb.org/), GeneCards database (https://www.genecards.org/, relevance score > 0), and DisGeNET (https://www.disgenet.org/, gene-disease association score ≥ 0.01). The search results were merged and duplicate targets were

removed to obtain the disease-related target set for CAG. The intersection of the potential target set of JFFW's active ingredients and the target set of CAG was identified as the core target of JFFW's treatment for CAG. Information on the drug composition, active ingredients, and core target of JFFW was compiled and imported into Cytoscape 3.10 software to construct a visual network topology diagram of "JFFW-CAG-Core Target". The CytoNCA plugin was used to perform topological analysis on the network, and key active ingredients of JFFW for treating CAG were selected based on topological feature values.

Construction of a protein-protein interaction (PPI) network: The core target was imported into the STRING database analysis tool (https://cn.string-db.org/) to construct a PPI network model. The parameters were set as follows: species selection: Homo sapiens; lowest confidence score ≥ 0.9. The completed PPI network model was imported into Cytoscape 3.10 software for visualization analysis and topological structure verification.

Gene ontology (GO) functional enrichment analysis and Kyoto encyclopedia of genes and genomes (KEGG) pathway enrichment analysis: The core target of JFFW for treating CAG was submitted to the DAVID database (https://david.ncifcrf.gov/), with Homo sapiens as the species. GO functional enrichment analysis and KEGG pathway enrichment analysis were performed. The enrichment analysis results were imported into an online bioinformatic visualization platform (https://www.bioinformatics.com.cn/) to create visualization charts.

Molecular docking validation: The protein structure of PI3K (ID: 1e7u) was retrieved from the Protein Data Bank (PDB) database (http://www.rcsb.org). The three-dimensional molecular conformation of the key active ingredient of JFFW was obtained from the TCMSP database. Autodock Tools 1.5.6, OpenBabel, and PyMOL 2.6 softwares were used to sequentially complete the pretreatment of target proteins and active ingredients, calculate molecular docking binding energies, and visualize the docking results.

Statistical analysis

All statistical analyses were performed with GraphPad Prism software (version 8.0.1). Quantitative data were expressed as mean ± standard deviation ($\bar{x}$ ± SD). The Shapiro-Wilk test was used to verify the normality of the data. For comparisons among multiple groups using ELISA, histopathologic scoring, and IHC quantification, one-way ANOVA was used, and Tukey's method was used for multiple comparisons between groups. For repeated measures data such as mouse body weight at different time points, two-way repeated measures ANOVA was used, and Bonferroni's method was used for comparisons between groups. A *p*-value < 0.05 was considered significant.

Result

Effects of JFFW on body weight, serum biomarkers, and systemic inflammation in CAG mice

The effects of JFFW on CAG was assessed by monitoring mouse body weight. Body weight fluctuations between groups indicated that, starting from week 4, the model group showed a significant decrease in body weight compared to the control group ($P < 0.001$). After the start of treatment, administration of JFFW (6.89 g/kg) or MLD (0.72 g/kg) induced body weight recovery, showing a significant difference compared to the model group from week 15 ($P < 0.001$) (**Figure 2A**). ELISA analysis showed that, compared to the control group, the serum PGI concentration and the PGI/PGII ratio were significantly decreased in the model group (both $P < 0.01$) (**Figure 2B-D**). Furthermore, the levels of inflammatory cytokines such as IL-6, IL-1β, and TNF-α were significantly increased (all $P < 0.001$) (**Figure 2E-G**). After six weeks of administration of JFFW and MLD, the levels of PGI/PGII ratio significantly increased ($P < 0.01$). Conversely, the levels of IL-6, IL-1β, and TNF-α significantly decreased (all $P < 0.01$). Overall, these results indicate that JFFW treatment can significantly improve the gastric mucosal atrophy phenotype in a mouse model of CAG.

Effects of JFFW on gastric mucosal morphology and histopathology in CAG mice

The efficacy of JFFW for treating CAG was evaluated by histologic analysis and pathological assessment of mouse gastric tissue using H&E staining. Macroscopic observation of gastric tissue revealed that, compared to the healthy control group, the gastric mucosa in the model

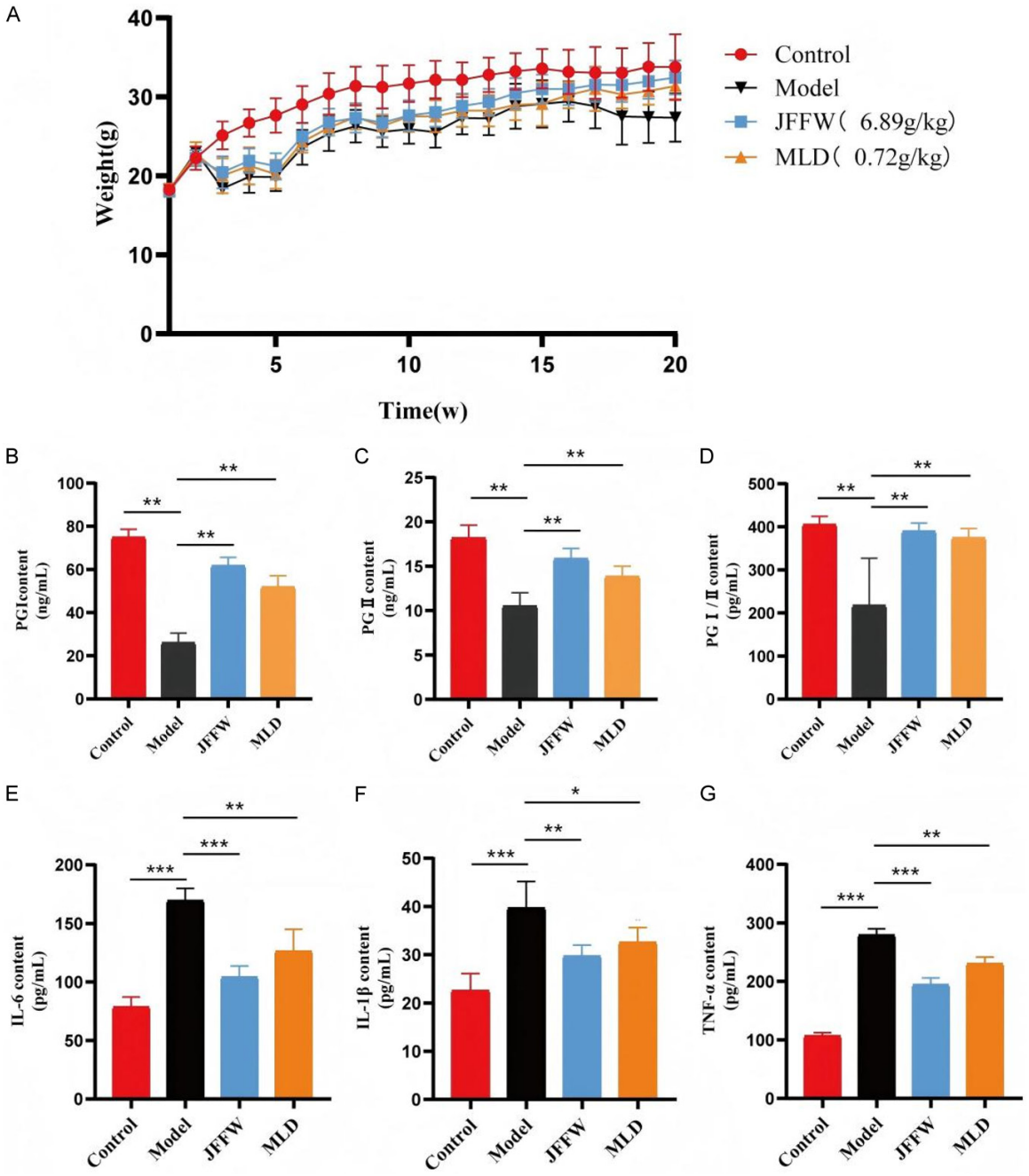

Figure 2. Effects of JFFW on body weight, pepsinogen, and inflammatory factors in CAG mice. (A) Changes in body weight of CAG mice over the 20-week experimental period. Statistical analysis for body weight was performed using two-way repeated measures ANOVA. (B) Serum levels of PGI, (C) PGII, and (D) the PGI/PGII ratio; Serum levels of inflammatory factors IL-6 (E), IL-1β (F), and TNF-α (G). Data are presented as mean ± SD (n = 7). Statistical significance for (B-G) was determined by one-way ANOVA followed by Tukey's post hoc test. Compared with the blank group, ***P < 0.001, **P < 0.01; compared with the model group, ***P < 0.001, **P < 0.01, *P < 0.05. Abbreviations: PGI: Pepsinogen I; PGII: Pepsinogen II; IL-6: Interleukin-6; IL-1β: Interleukin-1β; TNF-α: Tumor necrosis factor-α.

group was significantly paler, with fewer folds and a shallower inner wall. These symptoms were significantly improved after administration of JFFW and MLD (**Figure 3A**). Histopathologic analysis of gastric tissue showed that the gastric mucosal glands in the healthy control group were neatly arranged, with uniformly sized epithelial cells and no inflammatory cell

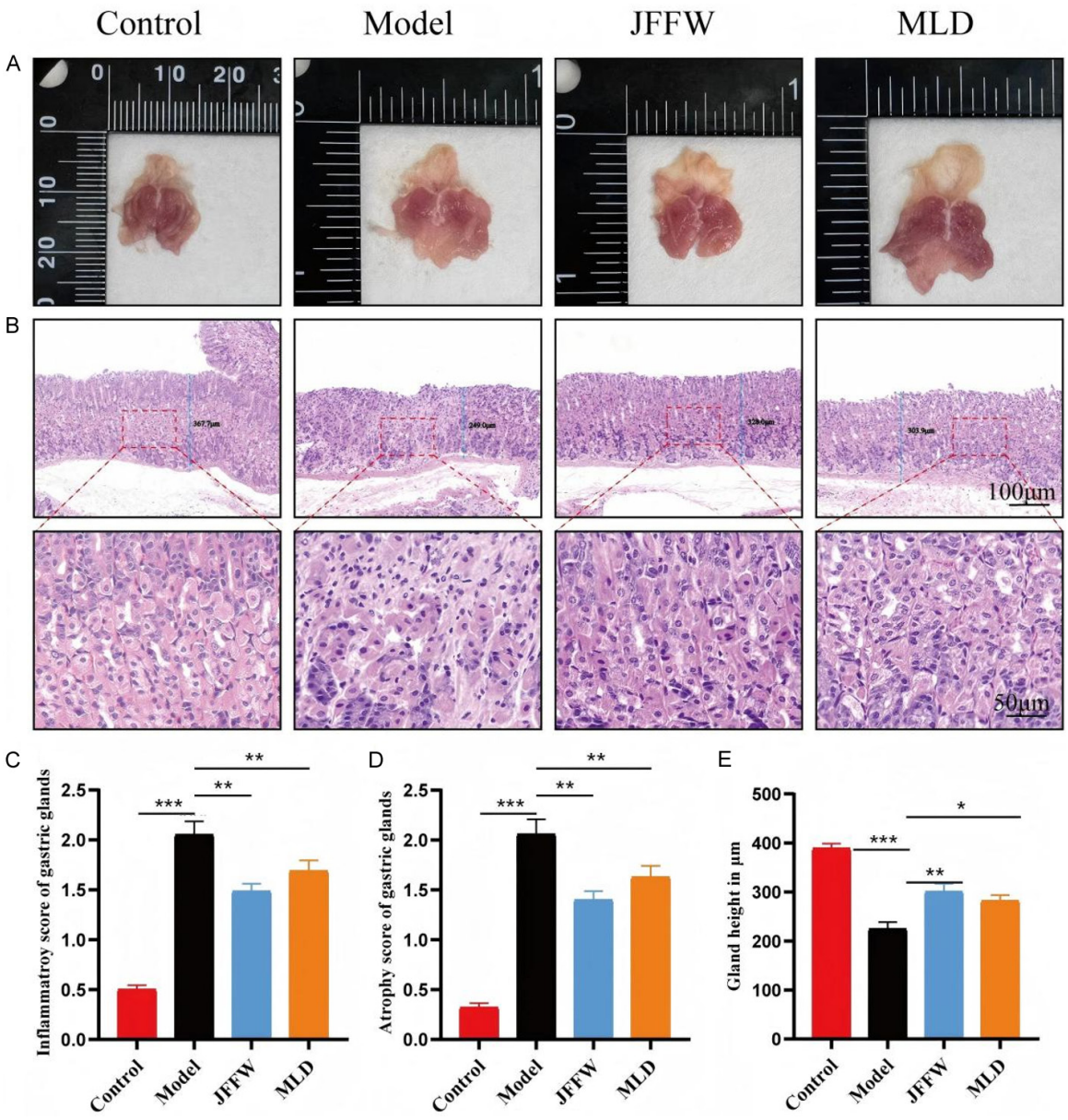

Figure 3. The effect of JFFW on gastric mucosal atrophy in CAG mice. (A) Gross appearance of the stomach in each group; (B) Representative H&E staining of gastric pathologic sections (first row magnification ×100, scale bar 100 μm; second row magnification ×200, scale bar 50 μm); (C) Inflammation scores, (D) Atrophy scores, and (E) Glandular height scores. Data were presented as mean ± SD (n = 7). Significance was assessed by one-way ANOVA followed by Tukey's post hoc test. ***P < 0.001, **P < 0.01, *P < 0.05. Abbreviations: CAG: Chronic atrophic gastritis; JFFW: Jiangfu Fuwei Granules; HE: Hematoxylin and eosin.

infiltration. Conversely, the model group exhibited a thinner gastric mucosa, with disordered and reduced glandular structure. Furthermore, significant inflammatory cell aggregation was observed in both the mucosal and submucosal layers. Compared to the model group, treatment with JFFW or MLD improved gastric mucosal atrophy and inflammatory lesions (**Figure 3B-E**).

Network pharmacology analysis

Acquisition of effective active components and potential targets of JFFW in treating CAG: From the TCMSP and STP databases, we retrieved a total of 224 active ingredients of JFFW, and subsequently identified 1086 related targets. In addition, we extracted 1,215 targets related to CAG from the OMIM, PharmGKB, DisGeNet,

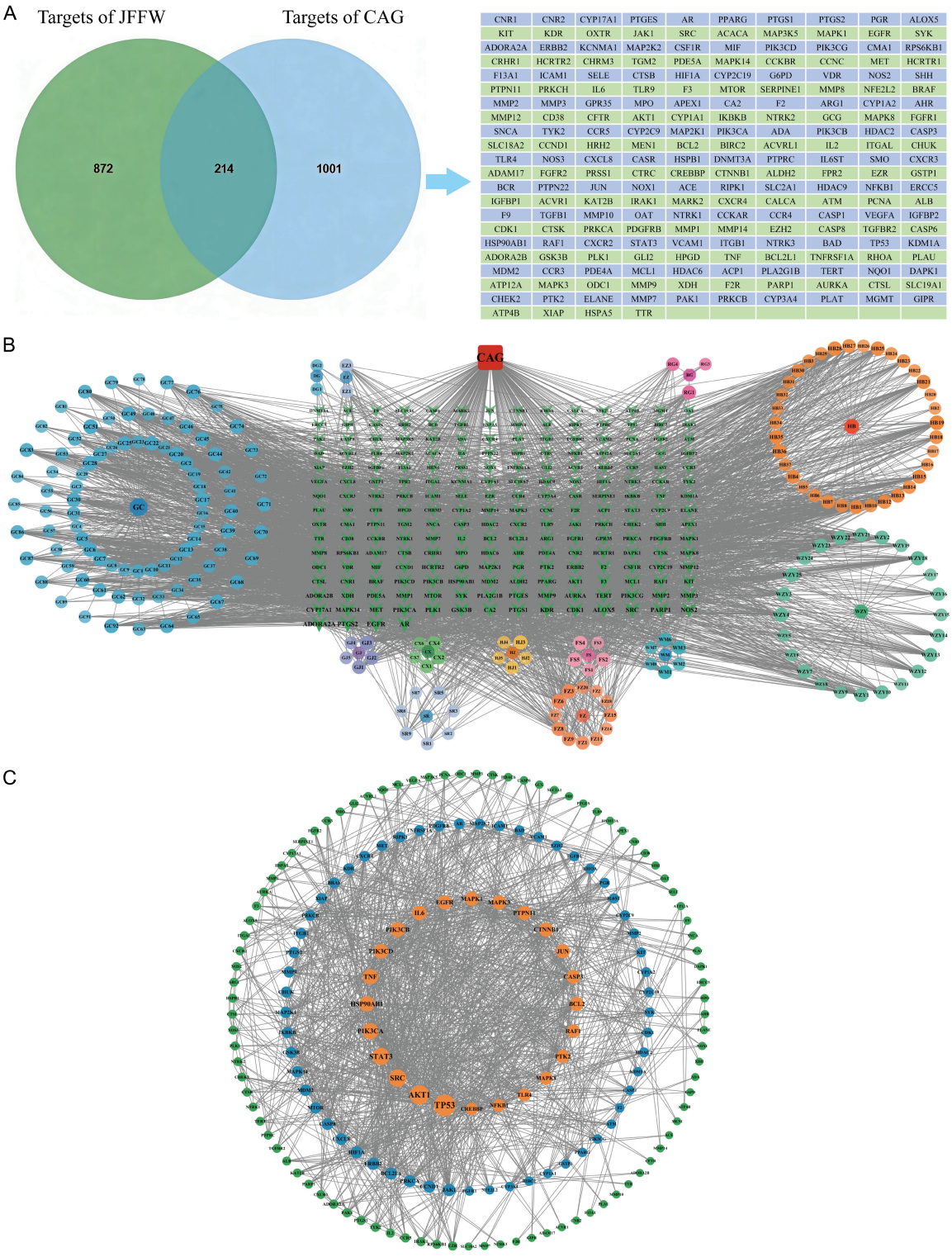

Figure 4. Preliminary analysis of the mechanism of JFFW in the treatment of CAG based on network pharmacology. A. Venn diagram. B. "JFFW-CAG-Target" network. C. PPI network. Abbreviations: FZ: Monkshood (Radix Aconiti Lateralis Preparata); GJ: Dried Ginger (Zingiberis Rhizoma); WZY: Evodia Rutaecarpa (Euodiae Fructus); HJ: Zanthoxylum Bungeanum (Zanthoxyli Pericarpium); RG: Cinnamomum Cassia (Cinnamomi Cortex); HB: Phellodendron Bark (Phellodendri Chinensis Cortex); SR: Amomum Fruit (Amomi Fructus); WM: Dark Plum (Mume Fructus); CX: Chuanxiong (Chuanxiong Rhizoma); FS: Bergamot (Citri Sarcodactylis Fructus); DG: Angelica Root (Angelicae Sinensis Radix); EZ: Zedoary (Curcumae Rhizoma); GC: Licorice (Glycyrrhizae Radix et Rhizoma).

Table 1. The key drug active ingredients in the "JFFW-CAG-target" network (the top 20 of degree value)

ID	Mol ID	Molecule Name	OB%	DL	Degree
GC51	MOL004908	Glabridin	53.25	0.47	39
GC28	MOL004835	Glypallichalcone	61.60	0.19	38
HB19	MOL002671	Candletoxin A	31.81	0.69	38
GC76	MOL004990	7,2',4'-trihydroxy-5-methoxy-3-arylcoumarin	83.71	0.27	36
GC20	MOL004814	Isotrifoliol	31.94	0.42	36
GC6	MOL002565	Medicarpin	49.22	0.34	36
GC49	MOL004905	3,22-Dihydroxy-11-oxo-delta(12)-oleanene-27-alpha-methoxycarbonyl-29-oic acid	34.32	0.55	35
FZ6	MOL002395	Deoxyandrographolide	56.30	0.31	35
GC22	MOL004820	kanzonols W	50.48	0.52	34
FZ3	MOL002392	Deltoin	46.69	0.37	34
FS5	MOL002917	5,2',6'-Trihydroxy-7,8-dimethoxyflavone	45.05	0.33	34
FS2	MOL013253	5,2',5'-Trihydroxy-6,7,8-trimethoxyflavone	37.49	0.43	34
GC74	MOL004988	Kanzonol F	32.47	0.89	33
GC71	MOL004978	2-[(3R)-8,8-dimethyl-3,4-dihydro-2H-pyrano[6,5-f]chromen-3-yl]-5-methoxyphenol	36.21	0.52	33
GC39	MOL004866	2-(3,4-dihydroxyphenyl)-5,7-dihydroxy-6-(3-methylbut-2-enyl)chromone	44.15	0.41	33
GC17	MOL004808	glyasperin B	65.22	0.44	33
GC7	MOL000354	isorhamnetin	49.60	0.31	33
WZY22	MOL004019	GoshuyuamideII	69.11	0.43	33
WZY18	MOL004004	6-OH-Luteolin	46.93	0.28	33
WZY4	MOL000354	isorhamnetin	49.60	0.31	33

In the table: "OB" means Oral Bioavailability; "DL" means Drug Like.

and GeneCards databases. Using Venny plot analysis of the intersection of these datasets, we identified 214 overlapping targets between JFFW and CAG, which are potential therapeutic targets of JFFW for treating CAG (**Figure 4A**).

Construction and analysis of the "drug-target-disease" network: A network diagram of "JFFW-CAG-Target" was constructed using Cytoscape 3.10 software (**Figure 4B**). In this diagram, squares represent disease names, octagons represent drug components, circles represent active drug ingredients, and green triangles represent intersecting targets. The degree values of network nodes were calculated and screened using the CytoNCA plugin. The five active drug ingredients with the highest degree values were Glabridin, Glypallichalcone, Candletoxin A, 7,2',4'-trihydroxy-5-methoxy-3-arylcoumarin, and Isotrifoliol, as detailed in **Table 1**.

Construction and analysis of the PPI network: A PPI network was constructed by analyzing 214 overlapping targets using the STRING database. Topological analysis of this network was performed using Cytoscape 3.10 software (**Figure 4C**). Target proteins were ranked according to their degree values, and the topological features of the top 15 target proteins are shown in **Table 2**.

GO and KEGG enrichment analyses: GO and KEGG enrichment analyses were performed on potential targets of JFFW for the treatment of CAG using the DAVID database. The results of the GO analysis indicated that the biological processes mainly included negative regulation of apoptosis, phosphorylation, and protein phosphorylation (**Figure 5A**). Cellular components mainly involved the plasma membrane, cell surface, and cytoplasm (**Figure 5A**). Molecular functions mainly included identical protein binding, protein serine/threonine kinase activity, and enzyme binding (**Figure 5A**). Furthermore, pathway enrichment analysis using the KEGG revealed that the main signaling pathways associated with the treatment of CAG using JFFW included cancer-related pathways, TNF signaling pathways, PI3K-Akt pathway, HIF-1signaling pathway, and vascular endothelial growth factor signaling pathway (**Figure 5B**). This was further supported by data from the KEGG database, the PI3K-Akt pathway was identified as the upstream regulatory pathway of HIF-1. Activation of the PI3K-Akt pathway further modulates the HIF-1 signaling pathway, thereby regulating the expression of

Table 2. The topological parameters of the target protein interaction (the top 15 of degree value)

NO	Name	Degree	Betweenness	Closeness
1	TP53	90	5547.5986	0.4369
2	AKT1	76	3130.8325	0.4293
3	SRC	64	2106.8228	0.4090
4	STAT3	62	2827.8303	0.4347
5	PIK3CA	54	968.7711	0.3986
6	TNF	50	2189.0176	0.4149
7	HSP90AB1	50	2290.0435	0.4071
8	PIK3CD	46	416.2536	0.3704
9	PIK3CB	46	416.2536	0.3704
10	IL6	44	3512.2358	0.4100
11	MAPK1	42	926.1345	0.4109
12	MAPK3	42	1015.0333	0.4119
13	CTNNB1	42	1011.3030	0.4014
14	EGFR	42	1029.4745	0.4033
15	PTPN11	42	2892.7039	0.3642

endothelial nitric oxide synthase and inducible nitric oxide synthase; both enzymes are involved in the regulation of vascular tension and angiogenesis level (**Figure 5C**).

Effects of JFFW on PI3K-AKT-HIF1α expression in gastric tissues of CAG mice

Our network pharmacology experiments revealed that the "PI3K-AKT-HIF1α" signaling pathway may play a critical role in JFFW treatment of CAG. To further validate this finding, we performed immunohistochemical analysis on mouse gastric tissue. The results showed that, compared to the control group, the levels of P-AKT and HIF-1α were significantly increased in the model group (both $P < 0.001$). After six weeks of JFFW treatment, the levels of P-AKT and HIF-1α in CAG mice were significantly decreased (both $P < 0.01$; **Figure 6A**, **6B**, **6D**, **6E**).

Effects of JFFW on MVD in gastric tissues of CAG mice

A comprehensive literature review of the HIF1 pathway indicates that HIF1 activation has a significant effect on angiogenesis. To validate this finding, we used immunohistochemistry to assess the number of blood vessels in the gastric tissue of mice in different experimental groups. The examination revealed a significant increase in MVD in the model group compared to the control group ($P < 0.001$). However, after four weeks of JFFW treatment, MVD significantly decreased ($P < 0.001$) (**Figure 6C**, **6F**).

Molecular docking results

We focused on key active pharmaceutical ingredients identified from the "JFFW-target-CAG" network: glycyrrhizin, evodiamide II, glycyrrhizin chalcone, deoxyandrographolide, 5,2',6'-trihydroxy-7,8-dimethoxyflavone, and hexamethylenetetramine. We performed molecular docking of these compounds with the PI3K protein and calculated their binding energies using AutoDock (see **Table 3**). The results are visualized in **Figure 7**. It is noteworthy that lower binding energies between compounds and target proteins indicated stronger stability, activity, affinity, and interaction forces.

Discussion

Globally, gastric cancer remains one of the most common malignant tumors and a leading cause of death. Chronic atrophic gastritis (CAG) has been identified as a precancerous lesion that can lead to gastric cancer and is also a fairly common digestive system disease with an estimated global prevalence of 10% to 30%. This condition is crucial for the prevention and control of gastric cancer, and such management should be carried out effectively [15]. TCM is characterized by its holistic approach and syndrome differentiation and treatment, and it has shown significant efficacy in the treatment of CAG. JFFW is a TCM compound developed by Professor Jiang Liyun (an academic successor of the Fuyang School of the Yunnan Wu), a famous TCM practitioner in Yunnan Province, based on the pathogenesis of CAG of spleen and kidney yang deficiency and liver cold qi stagnation. The formula has been applied for as a national patent prescription by the Third Affiliated Hospital of Yunnan University of TCM. JFFW has the effects of warming yang and tonifying deficiency, and can warm and tonify the spleen and kidney, warm the liver and stomach, and promote blood circulation and qi flow. It has been used in clinical practice for more than ten years to treat CAG. Nevertheless, the exact pharmacologic mechanism of JFFW in treating CAG is still unclear. In this study, we predicted the potential mechanism

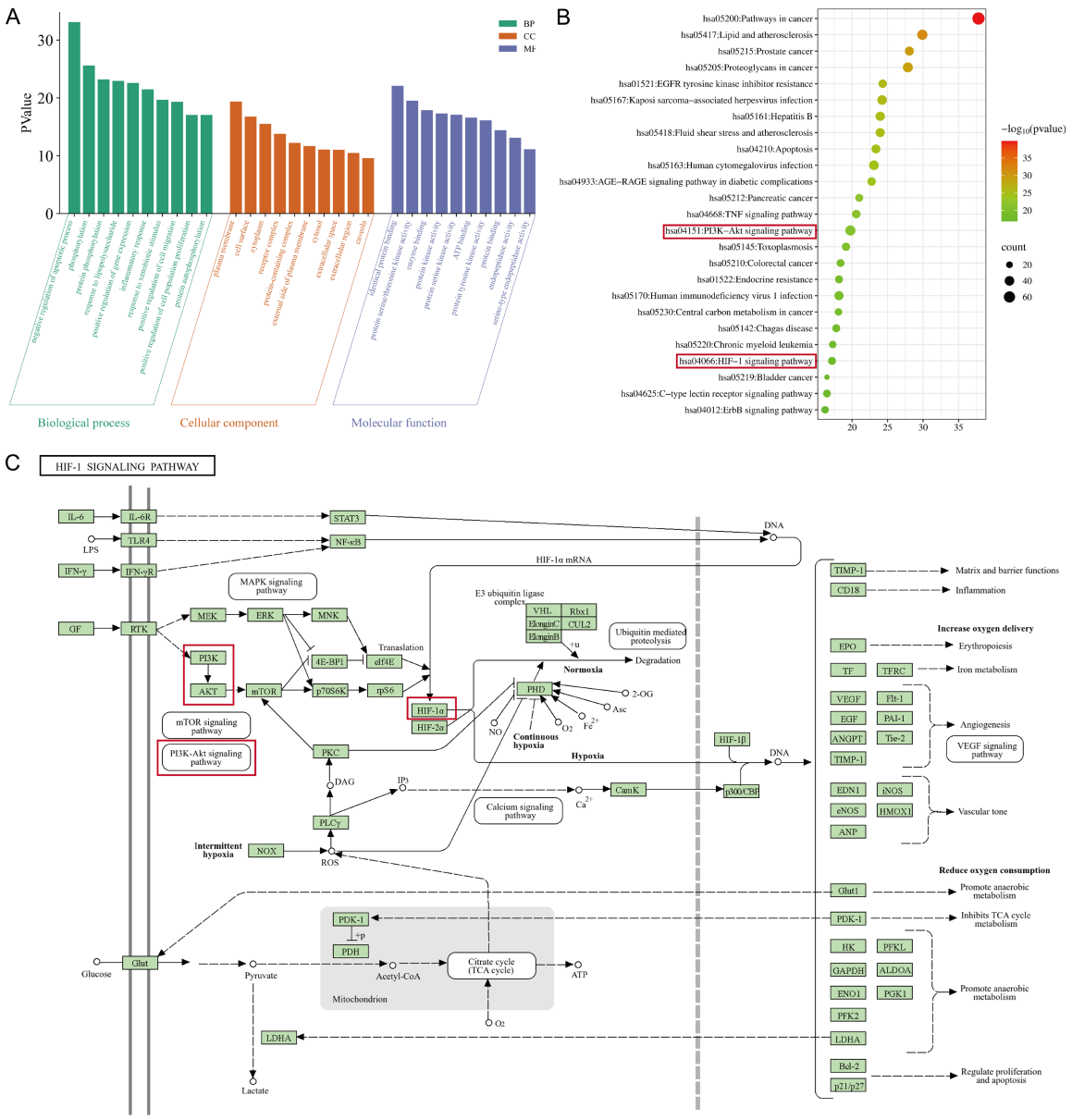

Figure 5. Enrichment analysis and gene-pathway network analysis. A. Top 10 GO terms of key genes. B. Top 30 KEGG terms of key genes. C. The MAP diagram of the HIF-1 signaling pathway. Abbreviations: GO: Gene Ontology; KEGG: Kyoto Encyclopedia of Genes and Genomes; HIF-1: Hypoxia-inducible factor 1.

of JFFW in treating CAG using network pharmacology and conducted *in vivo* experimental verification using an N-methyl-N'-nitro-N-nitrosoguanidine (MNNG) - induced CAG mouse model.

To investigate the positive effects of JFFW on CAG, we conducted a compound modeling study using mice. MNNG is an alkylating agent that mimics the ability of nitrates to be converted into carcinogenic compounds such as nitrosamines in the stomach which may induce CAG and potentially lead to gastric cancer [16]. Ranitidine has been reported to produce the carcinogen N-nitrosodimethylamine (NDMA), which is one of the causes of gastrointestinal cancer [17]. The stomach is one of the organs most negatively affected by alcohol intake. Drinking alcohol may lead to gastric mucosal erosion, gastric musculoskeletal dysfunction, and hypergastrinemia, which in turn can cause gastritis [18]. In addition, nonsteroidal anti-inflammatory drugs (NSAIDs), such as aspirin,

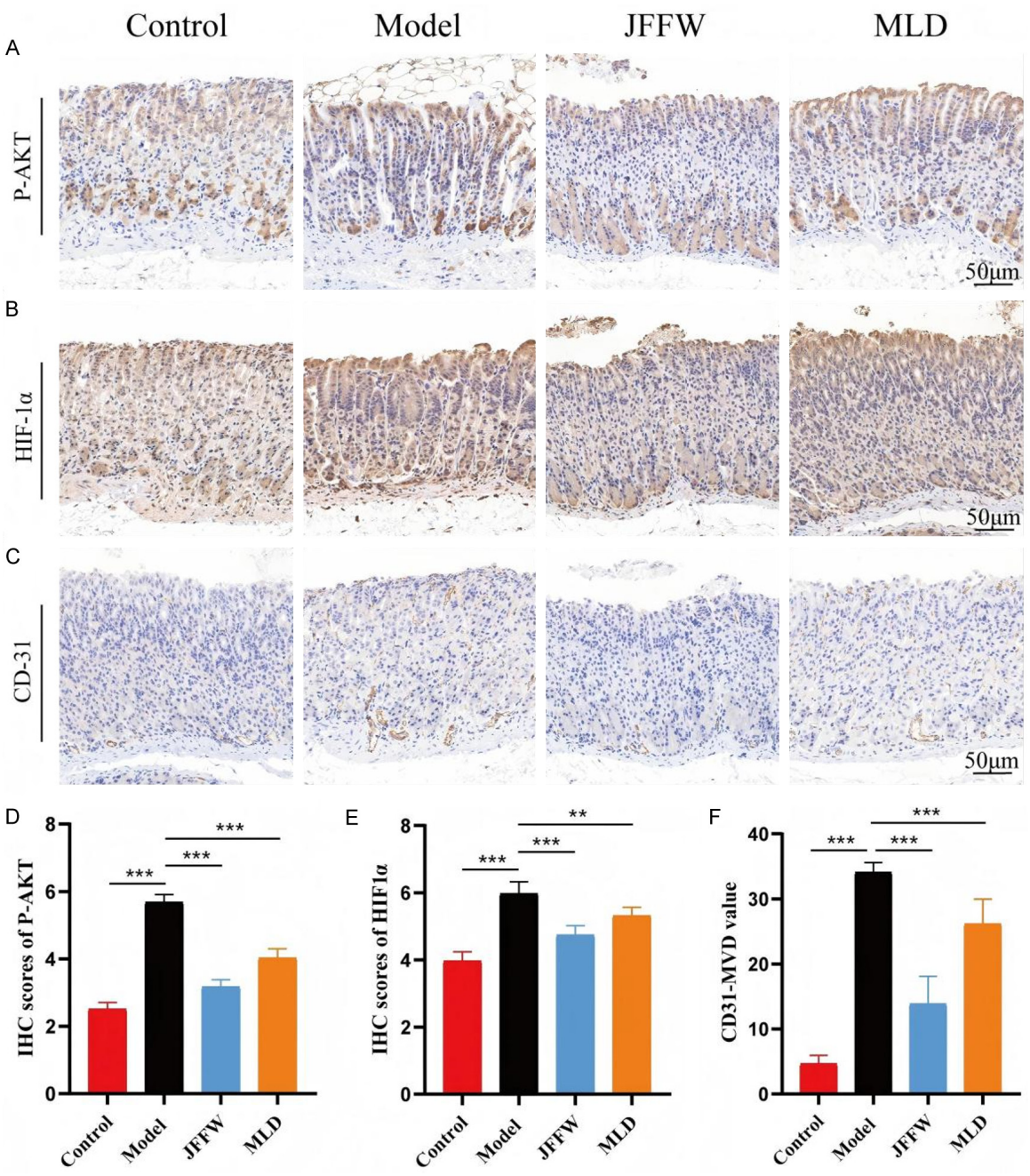

Figure 6. JFFW inhibits the expression of P-AKT and HIF-1α and suppresses angiogenesis in gastric tissues of CAG mice. (A) Representative immunohistochemical staining of P-AKT, (B) HIF-1α, and (C) CD31 proteins (scale bar = 50 μm). (D) Statistical quantification of P-AKT levels. (E) Statistical quantification of HIF-1α levels. (F) Statistical quantification of microvessel density (CD31-MVD). Data were presented as mean ± SD (n = 7). Abbreviations: CAG: Chronic atrophic gastritis; JFFW: Jiangfu Fuwei Granules; P-AKT: Phosphorylated Protein Kinase B; HIF-1α: Hypoxia-inducible factor 1-alpha; CD31: Cluster of differentiation 31. Significance was assessed by one-way ANOVA followed by Tukey's post hoc test. ***P < 0.001, **P < 0.01.

may also affect mucoprotein phospholipids or cell membranes, disrupting mitochondrial oxidative phosphorylation and causing mucosal damage [19]. This study established a CAG model in mice by allowing them free access to MNNG, intermittently administering ranitidine, and periodically gavage with a mixture of ethanol and salicylic acid [20-22]. Diagnosis and

Table 3. The binding energy of the key components with PI3K protein

NO	Components	Binding energy (kcal/mol)	Source
1	Glabridin	-8.74	GC
2	GoshuyuamideII	-7.05	WZY
3	Glypallichalcone	-6.74	GC
4	Deoxyandrographolide	-6.66	FZ
5	5,2',6'-Trihydroxy-7,8-dimethoxyflavone	-5.79	FS
6	Sexangularetin	-5.71	GJ

GC: Licorice; WZY: Evodia Rutaecarpa; FZ: monkshood; FS: Bergamot; GJ: Dried Ginger.

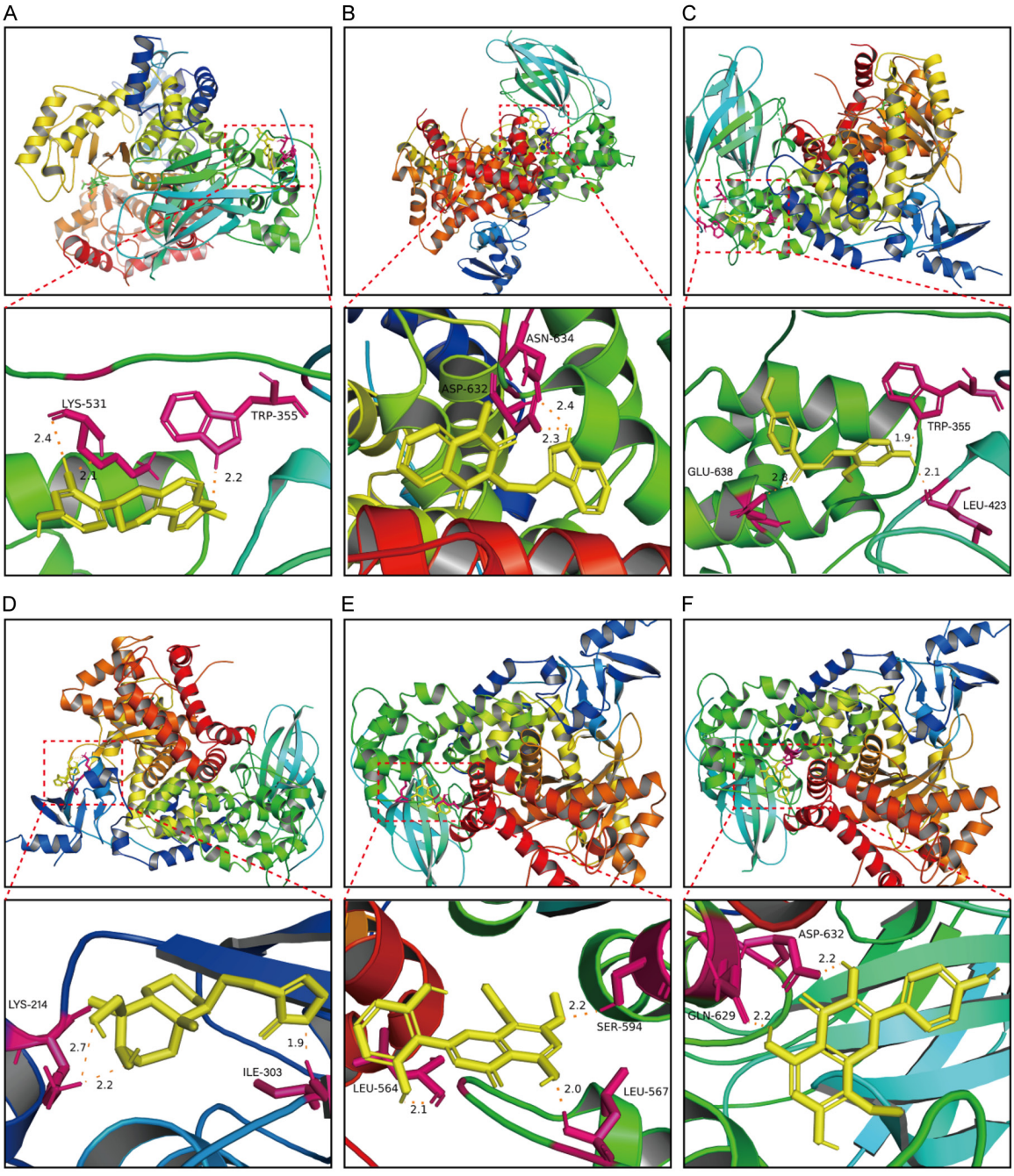

Figure 7. Molecular docking results of active ingredients of JFFW with PI3K protein. Glabridin (A), Goshuyuamide II (B), Glypallichalcone (C), Deoxyandrographolide (D), 5,2',6'-Trihydroxy-7,8-dimethoxyflavone (E), Sexangularetin (F). Abbreviations: JFFW: Jiangfu Fuwei Granules; PI3K: Phosphoinositide 3-kinase.

assessment of gastritis are primarily based on pathological symptoms and gastric function tests. The main indicators include pepsinogen I (PGI) and pepsinogen II (PGII). Chief cells and mucus neck cells in the gastric fundic glands are the main producers of PGI, while in different glands such as the antrum, fundus, and cardia, the mucus-secreting cells that constitute these glands produce large amounts of PGI. After passing through the gastric mucosa and being stabilized, pepsinogen enters the bloodstream; therefore, serum pepsinogen levels can be used to determine the number of glands and cells on the gastric mucosa, thereby assessing the pathologic state of the gastric mucosa [23]. Studies have shown that in CAG, gastric glandular cells and their atrophy lead to a decrease in PGI. Simultaneously, the replacement of normal gastrointestinal glands by pyloric glands or the occurrence of intestinal metaplasia also affects PGII levels [23, 24]. IL-6 and IL-1β are pro-inflammatory cytokines. IL-6 is an important cytokine that plays a crucial role in maintaining immunity and transmitting inflammatory signals [25]. Neutrophils, monocytes, macrophages, lymphocytes, and other cells can produce IL-1β. It plays an important role in regulating a variety of processes, including inflammatory immune damage, inhibiting gastric acid secretion, stimulating angiogenesis, and stimulating tumor cell metastasis, thereby playing a role in the transformation of gastritis into gastric cancer [26]. TNF-α plays a key role in many physiologic and pathologic processes, such as regulating immune responses during inflammation, inducing apoptosis, and playing a role in tumor development [27]. In our study, we found that JFFW can improve the pathologic changes of gastric mucosal tissue in mice with CAG. Furthermore, it can regulate excessive or insufficient PGI levels and the PGI/PGII ratio, and reduce the concentrations of inflammatory markers such as IL-6, IL-1β, and TNF-α in serum. This suggests that JFFW has the potential to actively improve gastric atrophy and inflammation in mice with CAG.

Subsequently, we predicted the mechanisms of action of JFFW and the substances it contains in the treatment of CAG. To identify the active compounds and targets of JFFW and CAG, we searched relevant databases. By constructing and analyzing drug-disease-target interaction networks using software, we found that the active ingredients of JFFW in treating CAG include glycyrrhizin, glycyrrhizin chalcone, Candletoxin A, 7,2',4'-trihydroxy-5-methoxy-3-arylcoumarin, and isotrichol. By constructing and evaluating PPI networks, we inferred that TP53, AKT1, SRC, and STAT3 may play important roles in this therapeutic process.

TP53 is a tumor suppressor gene that is most closely associated with human cancer. Mutations in this gene are particularly associated with cancer development and progression [28, 29]. Studies have shown that wild-type TP53 (WTP53) protein changes through phosphorylation or acetylation to form tetramers when cells are subjected to stresses such as hypoxia or injury. These tetramers can bind to p53 sites in the promoters and enhancers of target genes. WTP53 regulates a variety of processes through transcriptional regulation, including apoptosis [30, 31], ferroptosis [32], autophagy [33], and inhibition of tumor angiogenesis [34]. Serine/threonine protein kinase AKT1 activates related proteins, including MAPKs, thereby regulating cell proliferation, differentiation, migration, and cell death [35]. Recent studies have found that AKT1 regulates glucose metabolism in tumor cells by phosphorylating malate 2 (ME2) and hexokinase 1 (HK1) and hexokinase 2 (HK2) in the hexokinase family, thereby affecting tumor proliferation and metastasis [36, 37]. SRC is a non-receptor tyrosine kinase that, upon activation, interacts with growth factors, cytokines, steroid hormones, G protein-coupled receptors, and adhesion molecule receptors. This interaction activates signal transduction, significantly affecting cell growth, motility, differentiation, and survival [38]. The oxidative stress transcription factor STAT3 is involved in various biological processes, including activation and proliferation. Studies have also shown that the relationship between STAT3 and the transcription factor nuclear factor κB (NF-κB) leads to overactivation of NF-κB, which in turn promotes the production of various inflammatory fac-

tors and triggers inflammatory responses. Moreover, STAT3 can bind to the promoters of immune checkpoint receptors (PD-1, PD-L1, PD-L2), upregulating their expression and helping tumor cells evade detection by the immune system [39].

KEGG pathway enrichment analysis revealed that the PI3K-Akt and HIF-1 signaling pathways play crucial roles in JFFW treatment of CAG. The PI3K-Akt signaling pathway is involved in various biological events, including cell growth, programmed cell death, angiogenesis, and glucose metabolism [40]. Related experiments show that when stimulated by external factors, PI3K phosphorylates the cell membrane substrate PIP2, converting it into PIP3 [41]. This conversion activates Akt, which then participates in the proliferation and apoptosis of cancer cells through various downstream pathways [41]. Other studies have confirmed that activation of the PI3K/Akt signaling pathway leads to phosphorylation of nuclear transcription factors (i.e., nuclear factor κ light chain enhancers, NF-B, which activate B cells) and subsequent translocation to the nucleus, thereby increasing the production of inflammatory mediators [42]. Moreover, PI3K/Akt signaling may promote the synthesis of HIF-1α by activating mTOR [43].

HIF-1 is extremely common in humans and mammals and is an important mediator of cellular adaptation to hypoxic stress. It consists of two subunits, HIF-1α and HIF-1β [44]. Studies have shown that under hypoxic conditions, HIF-1α accumulates in the cytoplasm and then translocates to the nucleus, where it binds to HIF-1β to form a heterodimer. This heterodimer interacts with hypoxia response elements (HREs) on the promoters of HIF-1 target genes, thereby activating downstream target genes and regulating a range of biological processes, including angiogenesis, glucose metabolism, cell growth, and apoptosis [45-48]. Notably, HIF-1α is a key regulator of angiogenesis by vascular endothelial growth factor (VEGF). In addition to increasing vascular permeability, VEGF helps maintain endothelial cell survival, promotes their proliferation and migration. Therefore, activation of HIF-1 has a direct and significant effect on angiogenesis [44, 49]. CD31, the platelet endothelial cell adhesion molecule, is a specific marker of vascular endothelial cells. MVD is an effective parameter for measuring the level of microangiogenesis by counting CD31-labeled microvessels [50, 51]. Although angiogenesis is generally considered an adverse factor promoting tumorigenesis and metastasis, it contributes to the repair of the gastric mucosa in the early stages of CAG. However, as CAG progresses, angiogenesis may exacerbate malignant transformation [52]. Yang's research pointed out that the disordered changes of gastric mucosal glands in CAG model rats are related to the presence of neovascularization, which means that the degree of gastric gland imbalance is positively correlated with neovascularization [52].

Based on the results of our network pharmacology analysis, we speculate that the process and efficacy of JFFW in treating CAG may be mainly related to the above-mentioned targets and pathways. Molecular docking analysis of the main active ingredients and key targets of JFFW positive molecular interactions between them. This implies that these small molecule compounds may play a key role in the treatment of CAG. In addition, some literature reviews have reported that the components in JFFW are closely related to the PI3K-AKT-HIF-1α signaling pathway, such as dried ginger, Evodia rutaecarpa, Zanthoxylum bungeanum, and Chuanxiong. Dehydroevodiamine, the extract of Evodia rutaecarpa, can also regulate the level of oxidative stress, balance the oxidation and antioxidation processes, and prevent gastric mucosal damage [53]. Studies have shown that the flavonoids contained in dried ginger have strong antioxidant capacity [54], and dried ginger can be used to protect the gastric mucosa and inhibit tumor metastasis [12]. Studies have shown that Zanthoxylum bungeanum can inhibit the synthesis of inflammatory cytokines (tumor necrosis factor-α and interleukin-1β), thus it is an effective anti-inflammatory agent [55]. Chuanxiong has various pharmacological effects, including but not limited to anti-inflammatory, antioxidant, and vascular endothelial cell protective effects [56].

Based on the literature review and analysis results, we believe that the PI3K-AKT-HIF1 signaling pathway is crucial for the treatment of CAG with JFFW. Therefore, we chose to experimentally verify this pathway. By detecting the expression levels of P-AKT and HIF-1 and calculating MVD, we found that the expression P-

AKT and HIF-1, as well as the MVD of gastric tissue after modeling, all changed significantly. However, after six weeks of administration of JFFW, these conditions were significantly improved. Therefore, we can conclude that JFFW can downregulate the PI3K-AKT-HIF1 pathway, inhibit angiogenesis, and thus slow the progression of CAG to malignancy. This study, by exploring the molecular mechanism and efficacy of JFFW in treating CAG, provided valuable experimental evidence for its rational application in the treatment of CAG.

This study also had some limitations. First, the prediction of the main chemical components of JFFW based on the database was not comprehensive enough. We will reduce this bias by introducing subsequent innovative technologies and improving liquid chromatography-mass spectrometry analysis. Second, the network pharmacology analysis did not consider the possible formation of new compounds between drugs and the influence of component content, leading to a slight deviation between the analytical results and the actual situation. Finally, the results of the molecular docking experiment have not been verified by any experimental procedures. To further elucidate the mechanism of action of JFFW in treating CAG, we plan to conduct more experiments.

Conclusions

JFFW can downregulate the PI3K-AKT-HIF1α signaling pathway, block abnormal angiogenesis, and help delay or even reverse the malignant development of CAG. This study explored and verified the possible mechanism of action of JFFW for treating CAG, providing experimental evidence for its application in clinical practice.

Acknowledgements

We extend our heartfelt thanks to the personnel at the Central Laboratory of the Yunnan Provincial Hospital of Traditional Chinese Medicine for their significant support in carrying out this research. This work is supported by Science and Technology Plan Project of Yunnan Provincial Department of Education (2025Y0649); Yunnan Provincial Science and Technology Department Research Program (202401AT070010 and 202101AZ0700012-69); "Ten-Thousand Talents Plan" of Yunnan Province (No. YNWR-MY-2018-057).

Disclosure of conflict of interest

None.

Address correspondence to: Liyun Jiang, Department of Pi-Wei Disease, The Third Affiliated Hospital of Yunnan University of Chinese Medicine, No. 2628, Xiangyun Street, Kunming 650500, Yunnan, China. E-mail: liyunjiang20251116@163.com

References

[1] Li J, Pan J, Xiao D, Shen N, Wang R, Miao H, Pu P, Zhang H, Yv X and Xing L. Chronic atrophic gastritis and risk of incident upper gastrointestinal cancers: a systematic review and meta-analysis. J Transl Med 2024; 22: 429.

[2] Li JX, Chen C, Lyu B, Tang XD, Zhang SS, Li ZS, Wei W, Li YQ and Zhang ZQ. Consensus opinions on integrated traditional Chinese and Western medicine for chronic atrophic gastritis (2017). Chin J Integr Tradit West Med Dig [In Chinese] 2018; 26: 121-131.

[3] White JR and Banks M. Identifying the pre-malignant stomach: from guidelines to practice. Transl Gastroenterol Hepatol 2022; 7: 8.

[4] Huang RJ and Hwang JH. Improving the early diagnosis of gastric cancer. Gastrointest Endosc Clin N Am 2021; 31: 503-517.

[5] Fang JY, Du YQ, Liu WZ, Ren JL, Li YQ, Chen SY, Lu H, Min H and Lv NH. Chinese consensus on chronic gastritis (2017, Shanghai). Chin J Gastroenterol [In Chinese] 2017; 22: 670-687.

[6] Shah SC, Piazuelo MB, Kuipers EJ and Li D. AGA clinical practice update on the diagnosis and management of atrophic gastritis: expert review. Gastroenterology 2021; 161: 1325-1332, e7.

[7] Fang JY, Du YQ, Liu WZ, Ren JL, Li YQ, Chen SY, Lu H, Min H and Lv NH. Chinese guidelines for the diagnosis and treatment of chronic gastritis (2022, Shanghai). Chin J Gastroenterol [In Chinese] 2023; 28: 149-180.

[8] Chen L, He T, Wang R, Liu H, Wang X, Li H, Jing M, Zhou X, Wei S, Zou W and Zhao Y. Integrated approaches revealed the therapeutic mechanisms of Zuojin Pill against gastric mucosa injury in a rat model with chronic atrophic gastritis. Drug Des Devel Ther 2024; 18: 1651-1672.

[9] Liu Y, Huang T, Wang L, Wang Y, Liu Y, Bai J, Wen X, Li Y, Long K and Zhang H. Traditional Chinese Medicine in the treatment of chronic atrophic gastritis, precancerous lesions and gastric cancer. J Ethnopharmacol 2025; 337: 118812.

[10] Jiang L. A traditional Chinese medicine composition for treating gastric diseases and its application. Chinese patent CN109395047B. 2021.
[11] Zheng SC, Yan XY, Chen J, Zhao ST and Wen CB. Anti-inflammatory mechanism analysis of antirheumatic Chinese medicinal herb Aconiti Radix based on protein interaction network. Zhongguo Zhong Yao Za Zhi 2017; 42: 1747-1750.
[12] Ye N, Wang WS, Zhang HL and Wang ZX. Research progress on pharmacological effects and pharmacological effects of Ganjiang (Zingiberis Rhizoma). Chin Arch Tradit Chin Med [In Chinese] 2024; 42: 206-209.
[13] Zhao L, Zhang H, Li N, Chen J, Xu H, Wang Y and Liang Q. Network pharmacology, a promising approach to reveal the pharmacology mechanism of Chinese medicine formula. J Ethnopharmacol 2023; 309: 116306.
[14] Zhang P, Zhang D, Zhou W, Wang L, Wang B, Zhang T and Li S. Network pharmacology: towards the artificial intelligence-based precision traditional Chinese medicine. Brief Bioinform 2023; 25: bbad518.
[15] Thrift AP, Wenker TN and El-Serag HB. Global burden of gastric cancer: epidemiological trends, risk factors, screening and prevention. Nat Rev Clin Oncol 2023; 20: 338-349.
[16] Hu PJ, Yu J, Zeng ZR, Leung WK, Lin HL, Tang BD, Bai AH and Sung JJ. Chemoprevention of gastric cancer by celecoxib in rats. Gut 2004; 53: 195-200.
[17] Adami HO, Trolle Andersen I, Heide-Jørgensen U, Chang ET, Nørgaard M and Sørensen HT. Ranitidine use and risk of upper gastrointestinal cancers. Cancer Epidemiol Biomarkers Prev 2021; 30: 2302-2308.
[18] Liu J, Guo M and Fan X. Ethanol induces necroptosis in gastric epithelial cells in vitro. J Food Biochem 2021; 45: e13692.
[19] Seo PJ, Kim N, Kim JH, Lee BH, Nam RH, Lee HS, Park JH, Lee MK, Chang H, Jung HC and Song IS. Comparison of indomethacin, diclofenac and aspirin-induced gastric damage according to age in rats. Gut Liver 2012; 6: 210-217.
[20] Chu F, Li Y, Meng X, Li Y, Li T, Zhai M, Zheng H, Xin T, Su Z, Lin J, Zhang P and Ding X. Gut microbial dysbiosis and changes in fecal metabolic phenotype in precancerous lesions of gastric cancer induced with N-Methyl-N'-Nitro-N-nitrosoguanidine, sodium salicylate, ranitidine, and irregular diet. Front Physiol 2021; 12: 733979.
[21] Han L, Li T, Wang Y, Lai W, Zhou H, Niu Z, Su J, Lv G, Zhang G, Gao J, Huang J and Lou Z. Weierning, a Chinese patent medicine, improves chronic atrophic gastritis with intestinal metaplasia. J Ethnopharmacol 2023; 309: 116345.
[22] Yu C, Su Z, Li Y, Li Y, Liu K, Chu F, Liu T, Chen R and Ding X. Dysbiosis of gut microbiota is associated with gastric carcinogenesis in rats. Biomed Pharmacother 2020; 126: 110036.
[23] Fan YP, Ding CM, Niu AJ, Li Y and Zhao Z. The value of serum pepsinogen 1 and 2 in the diagnosis of gastric cancer. Int J Lab Med [In Chinese] 2013; 34: 3349-3350.
[24] Botezatu A and Bodrug N. Chronic atrophic gastritis: an update on diagnosis. Med Pharm Rep 2021; 94: 7-14.
[25] Kang S, Narazaki M, Metwally H and Kishimoto T. Historical overview of the interleukin-6 family cytokine. J Exp Med 2020; 217: e20190347.
[26] Yuan XY, Zhang Y, Zhao X, Chen A and Liu P. IL-1β, an important cytokine affecting Helicobacter pylori-mediated gastric carcinogenesis. Microb Pathog 2023; 174: 105933.
[27] Balkwill F. TNF-alpha in promotion and progression of cancer. Cancer Metastasis Rev 2006; 25: 409-416.
[28] Pan X, Ji X, Zhang R, Zhou Z, Zhong Y, Peng W, Sun N, Xu X, Xia L, Li P, Lu J and Tu J. Landscape of somatic mutations in gastric cancer assessed using next-generation sequencing analysis. Oncol Lett 2018; 16: 4863-4870.
[29] Peng Y, Bai J, Li W, Su Z and Cheng X. Advancements in p53-based anti-tumor gene therapy research. Molecules 2024; 29: 5315.
[30] Li M. The role of P53 up-regulated modulator of apoptosis (PUMA) in ovarian development, cardiovascular and neurodegenerative diseases. Apoptosis 2021; 26: 235-247.
[31] Ma S, Zhang H, Sun W, Gong H, Wang Y, Ma C, Wang J, Cao C, Yang X, Tian J and Jiang Y. Hyperhomocysteinemia induces cardiac injury by up-regulation of p53-dependent Noxa and Bax expression through the p53 DNA methylation in ApoE(-/-) mice. Acta Biochim Biophys Sin (Shanghai) 2013; 45: 391-400.
[32] Kang R, Kroemer G and Tang D. The tumor suppressor protein p53 and the ferroptosis network. Free Radic Biol Med 2019; 133: 162-168.
[33] Yeo SY, Itahana Y, Guo AK, Han R, Iwamoto K, Nguyen HT, Bao Y, Kleiber K, Wu YJ, Bay BH, Voorhoeve M and Itahana K. Transglutaminase 2 contributes to a TP53-induced autophagy program to prevent oncogenic transformation. Elife 2016; 5: e07101.
[34] Dohn M, Jiang J and Chen X. Receptor tyrosine kinase EphA2 is regulated by p53-family proteins and induces apoptosis. Oncogene 2001; 20: 6503-6515.
[35] Hers I, Vincent EE and Tavaré JM. Akt signalling in health and disease. Cell Signal 2011; 23: 1515-1527.
[36] Chen T, Xie S, Cheng J, Zhao Q, Wu H, Jiang P and Du W. AKT1 phosphorylation of cytoplas-

mic ME2 induces a metabolic switch to glycolysis for tumorigenesis. Nat Commun 2024; 15: 686.
[37] Yu Y, Wang S, Wang Y, Zhang Q, Zhao L, Wang Y, Wu J, Han L, Wang J, Guo J, Xue J, Dong F, Zhang JH, Zhang L, Liu Y, Shi G, Zhang X, Li Y and Li J. AKT1 promotes tumorigenesis and metastasis by directly phosphorylating hexokinases. J Cell Biochem 2024; 125: e30613.
[38] Bagnato G, Leopizzi M, Urciuoli E and Peruzzi B. Nuclear functions of the tyrosine kinase src. Int J Mol Sci 2020; 21: 2675.
[39] Hanlon MM, Rakovich T, Cunningham CC, Ansboro S, Veale DJ, Fearon U and McGarry T. STAT3 mediates the differential effects of oncostatin M and TNFα on RA synovial fibroblast and endothelial cell function. Front Immunol 2019; 10: 2056.
[40] Liu J, Li M, Chen G, Yang J, Jiang Y, Li F and Hua H. Jianwei Xiaoyan granule ameliorates chronic atrophic gastritis by regulating HIF-1α-VEGF pathway. J Ethnopharmacol 2024; 334: 118591.
[41] Jia FY, Gao SW, Ma JL, Yang Y, Zhang Y and Li J. Research progress on mechanism of traditional Chinese medicine in treating gastric cancer based on PI3K/Akt/mTOR signaling pathway. Global Traditional Chinese Medicine [In Chinese] 2022; 15: 165-172.
[42] Balwani S, Chaudhuri R, Nandi D, Jaisankar P, Agrawal A and Ghosh B. Regulation of NF-κB activation through a novel PI-3K-independent and PKA/AKT-dependent pathway in human umbilical vein endothelial cells. PLoS One 2012; 7: e46528.
[43] Kim D, Khin PP, Lim OK and Jun HS. LPA/LPAR1 signaling induces PGAM1 expression via AKT/mTOR/HIF-1α pathway and increases aerobic glycolysis, contributing to keratinocyte proliferation. Life Sci 2022; 311: 121201.
[44] Zhao Y, Xing C, Deng Y, Ye C and Peng H. HIF-1α signaling: essential roles in tumorigenesis and implications in targeted therapies. Genes Dis 2023; 11: 234-251.
[45] Mahon PC, Hirota K and Semenza GL. FIH-1: a novel protein that interacts with HIF-1α and VHL to mediate repression of HIF-1 transcriptional activity. Genes Dev 2001; 15: 2675-2686.
[46] Kierans SJ and Taylor CT. Regulation of glycolysis by the hypoxia-inducible factor (HIF): implications for cellular physiology. J Physiol 2021; 599: 23-37.
[47] Ho PC, Bihuniak JD, Macintyre AN, Staron M, Liu X, Amezquita R, Tsui YC, Cui G, Micevic G, Perales JC, Kleinstein SH, Abel ED, Insogna KL, Feske S, Locasale JW, Bosenberg MW, Rathmell JC and Kaech SM. Phosphoenolpyruvate is a metabolic checkpoint of anti-tumor T cell responses. Cell 2015; 162: 1217-1228.
[48] Peng G and Liu Y. Hypoxia-inducible factors in cancer stem cells and inflammation. Trends Pharmacol Sci 2015; 36: 374-383.
[49] Zhu CH and Lyu GQ. Effects of Yiqi Huayu Jiedu method on serum PGI/PGII, HIF-1α, and VEGF levels in elderly patients with Hp-related chronic atrophic gastritis. Chin J Gerontol [In Chinese] 2022; 42: 573-577.
[50] Woodfin A, Voisin MB and Nourshargh S. PECAM-1: a multi-functional molecule in inflammation and vascular biology. Arterioscler Thromb Vasc Biol 2007; 27: 2514-2523.
[51] Pei SF, Zhao XQ, Zhang XD, Li Y and Wang J. Expression of B7-H3, CD31-MVD and EGFR in colorectal cancer tissues and their clinical significance. Pract J Cancer [In Chinese] 2025; 40: 1070-1072.
[52] Yang HB. Study on the regulation of Weiyan I on NF-κB/HIF-1α pathway in gastric mucosa of rats with atrophic gastritis. Guangzhou: Guangzhou University of Chinese Medicine 2015. [In Chinese].
[53] Wan J and Bao QC. Protective effect of dehydroevodiamine on gastric mucosa of rats with experimental gastric ulcer and its mechanism. Chin Tradit Herb Drugs [In Chinese] 2022; 42: 573-577.
[54] Li SM, Wang LR, Zhang WD and Li J. Study of extraction and antioxidation activity of flavonoid from zingiberis rhizoma. Food Ind [In Chinese] 2015; 36: 141-143.
[55] Zhang ZC. Protective effects and mechanisms of different extracts of Zanthoxylum bungeanum on model mice with ulcerative colitis. Ji-Lin: Jilin University 2017. [In Chinese].
[56] Guan YM, Jiang C, Zang ZZ, Wu WT, Zhu WF, Jin C, Wu X and Chen LH. Research progress on chemical constituents, pharmacological effects, and clinical applications of volatile oil from Chuanxiong (Ligusticum chuanxiong Hort.). Chin Tradit Pat Med [In Chinese] 2024; 46: 873-880.